Actin Adsorbed on HOPG and Mica Substrates: Characterization and Manipulation by Atomic Force Microscopy

D.V. Nicolau[*], G. S. Watson[**], C. Cahill[**], J. Blach[**] and S. Myhra[**]

[*]Swinburne University of Technology, PO Box 218, Hawthorn, VIC 3122, Australia
[**]School of Science, Griffith University, Nathan, QLD 4111, Australia

ABSTRACT

Actin deposited onto a hydrophobic graphite surface forms paracrystalline rafts consisting of F-actin filaments. Those filaments retain their internal coherence during manipulation by an atomic force microscope tip. However, the filaments can be 'herded' systematically in a direction perpendicular to their long axis, due to weak interaction with the substrate. Actin deposited onto a hydrophilic mica surface, on the other hand, tend to become immobilized due to strong out-of-plane interactions. Circular ordered actin features can be formed at preferred sites defined by the intersection of interfaces at micro-bubbles with the substrate. The observations may have applications for devices based on dynamics of molecular motors.

Keywords: actin, atomic force microscope

1 INTRODUTION

Actin is an essential constituent in systems and processes that are involved with muscle contraction, cell division and some pathological conditions (Somlyo et al. 2000) Accordingly the structure and function of actin has been receiving increasing attention due to its future nano-biotechnological roles in devices and processes, in particular those that aim to exploit the capabilities of molecular motors. The project has investigated 'paracrystalline rafts' of actin adsorbed onto graphite. As well, selective adsorption with nano-scale definition has been obtained on mica by taking advantage of the propensity of actin to seek sites of lowest energy configuration at interfaces.

2 METHODS

Frozen G-actin stock was thawed rapidly in DI H_2O at 37°C. Polymerizing was initiated in 5 mM potassium phosphate buffer at pH 7.5 with 100 mM KCl and 0.25 mM Mg ATP. The incubation took place at 37°C for 30 min. The incubated solution was spun at 45 Krpm for 60 min at RT, whereupon the supernatent was decanted. The actin pellet was then rinsed/washed in a buffer solution of 10 mM imidazole at pH 6.8, 40 mM KCl, 1 mM $MgCl_2$, and 0.5 mM DTT. Additional buffer was added for storage overnight at 4°C. The F-actin was then resuspended, resulting in a stock solution of 6 mg/mL.

Two dilutions were carried out, resulting in 0.06 mg/mL (S1) and $6x10^{-4}$ mg/mL (S2). Drops of 5 – 25 µL from S1 or S2 were placed on substrate surfaces and allowed to dry at RT (ambient humidity ca. 60%).

Two substrates were employed during the present study. Highly oriented pyrolytic graphite (HOPG) will present an atomically flat hydrophobic surface with sp^2 bonding. Clean surfaces were prepared by cleavage immediately before exposure to solution. Mica will likewise present an atomically flat surface composed of a silicate tetrahedral network. That surface is hydrophilic and will be covered with an adsorbed thin aqueous layer. Hydroxylation will then take place, thus generating a negative surface charge. However, ion exchange with the divalent cation ($K^+ \Leftrightarrow Mg^{2+}$) in the aqueous phase is likely to produce a positive surface charge density.

The AFM analysis and tip-induced manipulation were carried out with a JEOL JSPM-4200 multi-technique/multi-mode instrument under air ambient conditions. Imaging was performed in the constant force contact mode. Beam-shaped probes with nominal force constants of 0.06 and 0.58 N/m were used.

3 RESULTS AND DISCUSSION

Deposition of S1 actin on a hydrophobic HOPG substrate resulted in formation of paracrystalline rafts, Fig. 1, consisting of filamentary strands with longitudinal integrity being aligned at spacings of ca. 200 nm. The structures exhibited superficial resemblance to those reported in an earlier study by Shi et al. (2001). However, closer inspection in combination with the outcome of tip-induced manipulation has revealed distinct differences.

The spacing between the parallel rows was a factor of 4-5 greater than those of the earlier study. That study was based on transferring a self-assembled bi-layer consisting of a lipid monolayer and an F-actin layer onto a DPPC coated mica substrate (or an aged carbon-coated grid for EM analysis). The repeat distance perpendicular to the longitudinal structure was ascribed to the nodal distance, ca. 36 nm, along the double-stranded F-actin chain. The present ripple spacing must therefore have a different origin. The spacing between rows in Fig. 1 was found to be

a function of interaction with the tip. The dependence is illustrated in Fig. 2 by the break in order at the edge of a second scan over a smaller field of view.

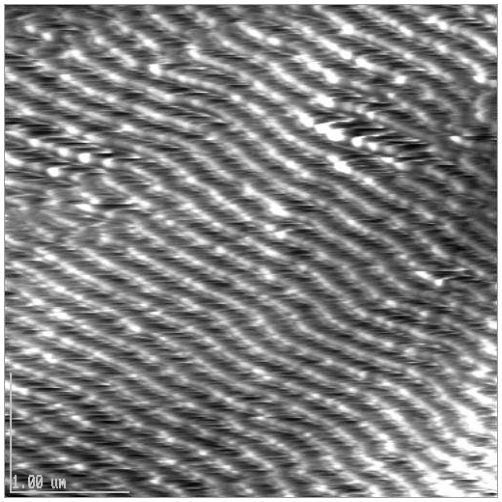

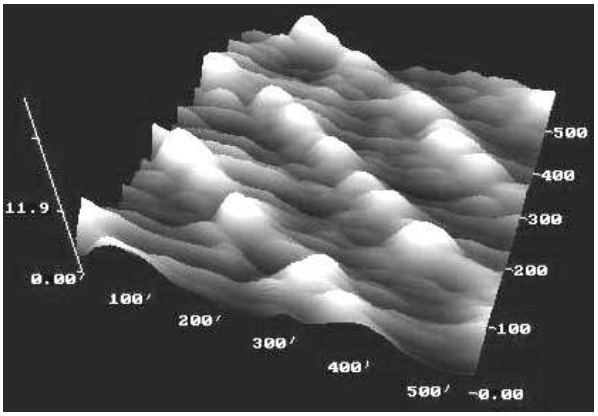

Fig. 1. Paracrystalline structure obtained from deposition of actin in S1 solution onto HOPG. The high-resolution image (right) reveals that the height (ca. 10 nm) and periodicity (ca. 40 nm) were consisted with SEM results for F-actin (Milligan et al. 1990).

Manipulation appeared to result in successive 'herding' of alternate strands, due to the delicate interplay of tip-induced shear stress, with in-plane and out-of-plane interactions within the raft and with the substrate.

Adsorption onto HOPG has the merit of effectively turning off double-layer interaction between the actin and the substrate. However, while HOPG is hydrophobic, the actin will be hydrophilic and will present a negative 'surface' charge. Thus ordering and spacings will be due to a subtle interplay between relatively weak and short-range out-of-plane van der Waals interaction with the substrate, longer-range in-plane repulsive electrostatic interaction, and attractive in-plane meniscus forces.

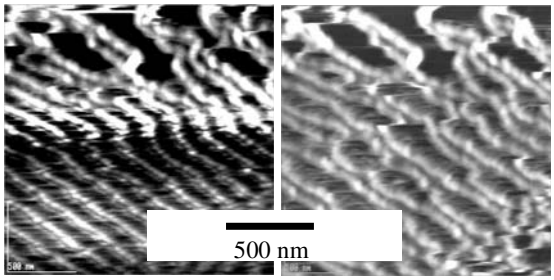

Fig. 2. The two contact mode images show: (left) the boundary between two successive scans over over-lapping fields of view, where the top half has been subjected to two raster scans, resulting in translation of every second row; (right) a third scan has been carried out over the full field of view, illustrating translation of every second row over the full field of view (note that the structure due to the original manipulation remained stable, top half of image).

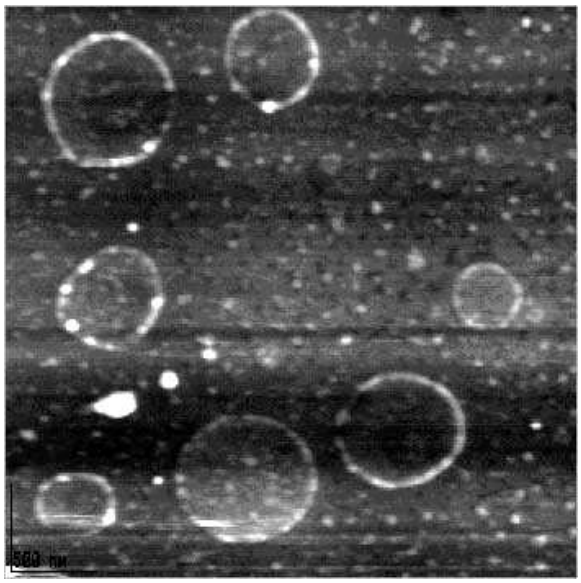

Fig. 3. Circular structures obtained from exposure of a hydrophilic mica surface to actin in S2 solution. The features are due to selective deposition of actin at preferred sites of low interface energy. Those sites are most likely located at the air/fluid/solid intersection where an adhering air bubble is attached to the mica surface. The existence of such bubbles is thought to account for anomalies in double-layer interactions (Considine et al. 1999). The features are stable against contact mode tip-manipulation, due to the double-layer force between a substrate with positive surface charge and a negative charge on the actin (St-Onge and Gicquaud, 1989).

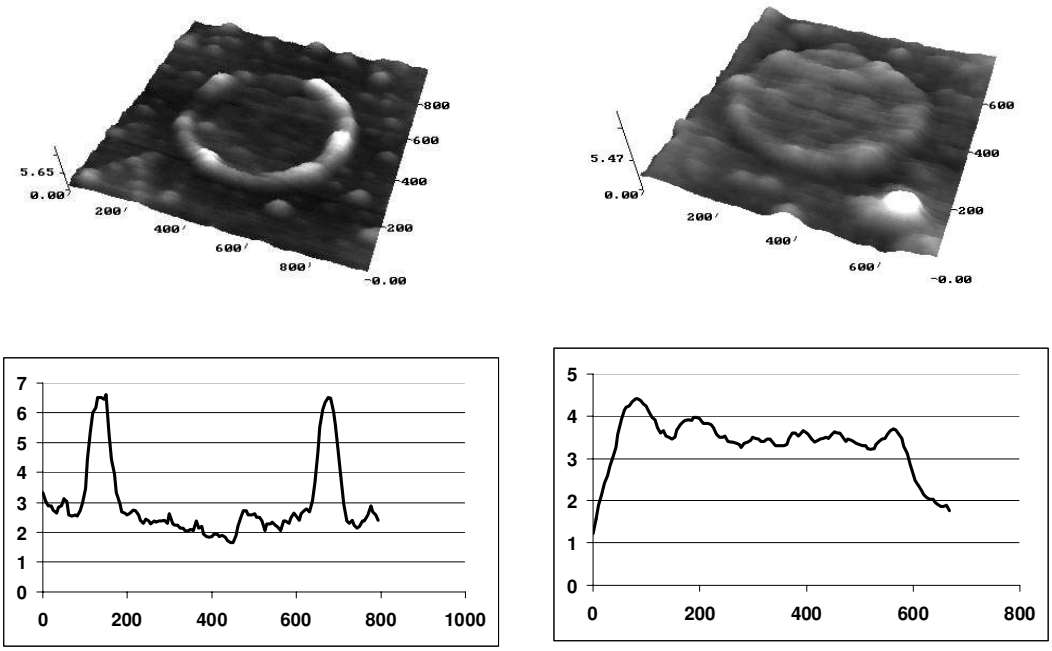

Fig. 4. Higher resolution images of circular features on mica shown in pseudo-3D representation. Most of the features exhibited adsorption along a 'triple-point' line (left). However, in some cases the circles were filled in (right), presumably due to availability of excess actin being forced into the circular confinement during evaporation. The contour lines are drawn through the center of the circle. The scales are in nm, and the heights of the features are consistent with that of a single layer of partially denatured actin.

4 CONCLUSIONS

Filamentary structures on a hydrophobic substrate form paracrystalline rafts that can readily be manipulated on the nano-scale, while adsorption on a hydrophilic surface suggests that tailored preferred adsorption sites at interfaces can be used to impose structural predictability. Both effects may have applications for nano-biotechnology.

REFERENCES

[1] Considine RF, Hayes RA, Horn RG, Langmuir, 15: 1657-1659, 1999
[2] Milligan RA, Whittaker M, Safer D, Nature, 348: 217-221, 1990
[3] Shi D, Somlyo A V, Somlyo A P, Shao Z, J. Microsc. 201: 377-382, 2001
[4] Somlyo AP, Somlyo AV, J. Physiol.-London 522: 177-185, 2000
[5] St-Onge D, Gicquaud C, Cell. Biol. 67: 297-300, 1989